P3.5

NUMERICAL SIMULATION OF ATMOSPHERIC TURBULENCE WITHIN AND ABOVE A CUBICAL CANOPY

Atsushi Inagaki *, Marieta Cristina L. Castillo, Yoshimi Yamashita and Manabu Kanda
Tokyo Institute of Technology, Tokyo, Japan

1. INTRODUCTION

We investigated the relationship between the flow structures within and above the building canopy under atmospheric conditions using numerical simulation. The motivation is to understand the scalar dispersion process within a building canopy and also the mechanism of the scalar and momentum exchange within and above the canopy layer. The main focus of this study is the nature of the instantaneous flow structures within the building canopy, which is different from their mean flow structure (e.g. Uehara et al. 2000; Kanda et al. 2004). Eliasson et al. (2006) observed in their urban field experiment that the number of vortices in a building cavity changes from time to time.

To study the characteristics of the instantaneous flow structure, some studies have reiterated the importance in considering the coherent structure of turbulence. Within an instantaneous flow field of inertial sublayer over a cubical array, very large coherent structure of turbulence has been observed experimentally (e.g. Inagaki and Kanda 2010) and numerically (e.g. Kanda et al. 2004, Coceal et al. 2007, Castillo et al. 2010). The observed structures are much larger than the size of the roughness cubes in the horizontal extent, and they have a main contribution to the vertical transport of momentum and heat in the inertial sublayer. Vertical distribution of the coherent turbulence has also been observed in urban field experiments (e.g. Oikawa and Meng 1995; Christen et al. 2007). The contribution of these structures penetrates into the canopy layer. These evidences imply that the coherent structures of turbulence developed in the inertial sublayer possibly contribute to the flow field within the canopy layer beyond the spatial scale of individual buildings or cavities.

Therefore, we investigated the contribution of the coherent structures of turbulence, which is developed within the inertial sublayer, on the instantaneous flow structure within the cubical canopy by using the large eddy simulation (LES) model. The numerical simulation allows us to investigate the three-dimensional flow structure in the canopy layer.

* *Corresponding author address*: Atsushi Inagaki, Tokyo Institute of Technology, Dept. of International Development Engineering, Meguro-ku, O-okayama, 2-12-1 I4-9 Tokyo, 152-8552 JAPAN; e-mail: inagaki.a.ab@m.titech.ac.jp

2. NUMERICAL SIMULATION

2.1 *PALM*

The atmospheric boundary layer (ABL) is simulated using PALM (Raasch and Schröter, 2001). This model can simulate the convective ABL with explicitly resolving the building geometry (Letzel 2007). PALM solves the filtered Navier-Stokes equation with non-hydrostatic assumption and incompressible Boussinesq approximation. The second moments of turbulent quantities are modeled following the Smagorinsky model. Flow around massive obstacles is explicitly resolved by using a mask method (Briscolini and Santangelo 1989; Kanda et al. 2004). Detail description of the model is found in Letzel (2007) and Castillo et al. (2010).

2.2 *Numerical settings*

The same simulation result has been used in the report by Castillo et al. (2010), in which the flow field includes the canopy layer of building array, which is simplified to a regular array of cubes, and the convective mixed layer above it. To simulate these layers simultaneously, we employed a large domain size (2560 m x 2560 m x 1709.6 m) with a fine grid spacing (dx=dy=dz=2.5 m) to explicitly resolve the flow around the roughness cubes whose height is 40 m (=H). Above the height of 1200 m, the vertical grid spacing is stretched by a factor of 1.08. The cubes are aligned regularly with the plan area index of 0.25. The mean flow regime in the building cavity of this setting is classified into the skimming flow regime (Oke 1987). The schematic of the computational domain is shown in Figure 1.

The mixed layer convection is invoked by sensible heat flux released from the roof and ground surfaces with a constant value (0.1 K m s^{-1}) and no heat flux from any vertical walls. The initial potential temperature gradient is 0.08 K m^{-1} below 800 m and

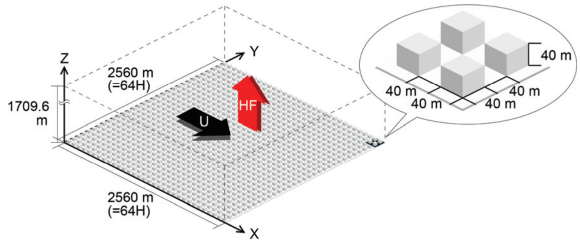

Figure 1 Schematic of the computational domain

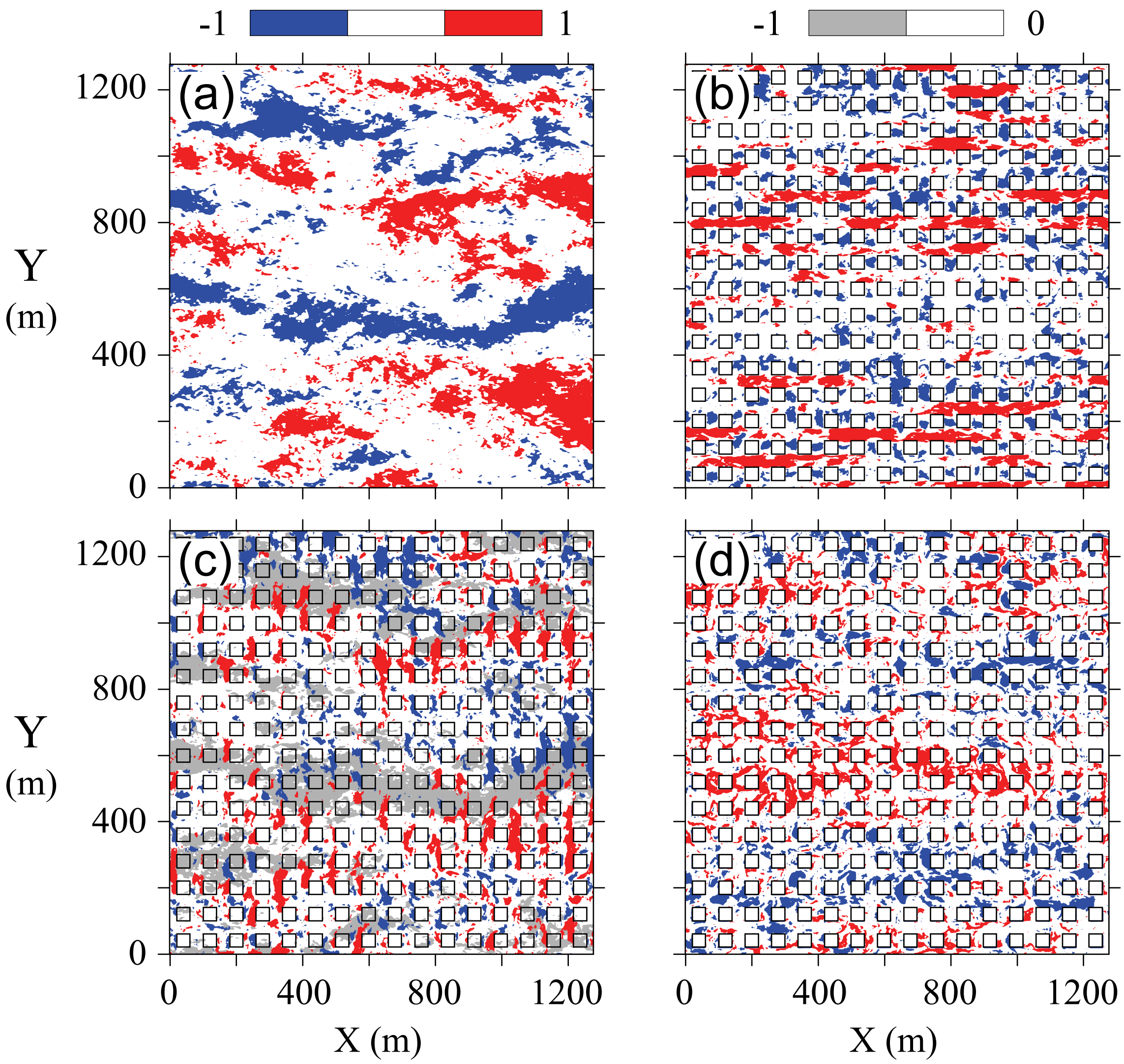

Figure 2 Horizontal distribution of velocity and temperature fluctuations at a quarter of the whole domain. (a) u' at z=2H, (b) u' at z=0.125H, (c) v at z=0.125H with negative u' at z=2H (gray area), (d) T' at z=0.125H.

0.74 K m^{-1} above 800 m to set the capping inversion.

The simulated turbulent statistics within the inertial sublayer and those in the convective mixed layer follow their respective similarity laws as confirmed by Castillo et al. (2010). The mean flow structure within the canopy layer is similar to that observed in wind tunnel experiments (e.g. Uehara et al., 2000).

3. CONTRIBUTION OF THE COHERENT TURBULENCE IN INERTIAL SUBLAYER

Figure 2 shows the horizontal distribution of u at 2H, and u, v, T at 0.125H from the ground, which are fluctuations from the horizontal average. In the distribution of u at 2H, we can see very large scale motion of high and low momentum regions elongated along the streamwise (x-) direction. The size of the structure is much larger than a cube. Inagaki and Kanda (2008, 2010) indicated that these are the characteristic structures of turbulence accounting for the inner-layer similarity law.

Comparing the distributions of u at 2H and 0.125H (Figure 2a, b), both high and low speed regions at 0.125H are mainly found below the high speed regions at 2H, and they are rarely observed below the low speed regions. The coherent structures of higher velocity regions at 2H drag the bottom air in the canopy along the x-direction. It accelerates the streamwise velocity in the street area along x, and enhances the curling motion behind the cubes (so-called, cavity vortex) which is seen as a backward motion at the bottom of the cavity.

Although the distribution of v at 0.125H (Figure 2c) is coherent along y-direction and separated in x-direction by cubes, the individual coherent v structures seem to form a cluster in which spanwise velocities direct the same way. These coherent clusters are much larger than cubes in the y-direction. The locations and directions of these clusters are

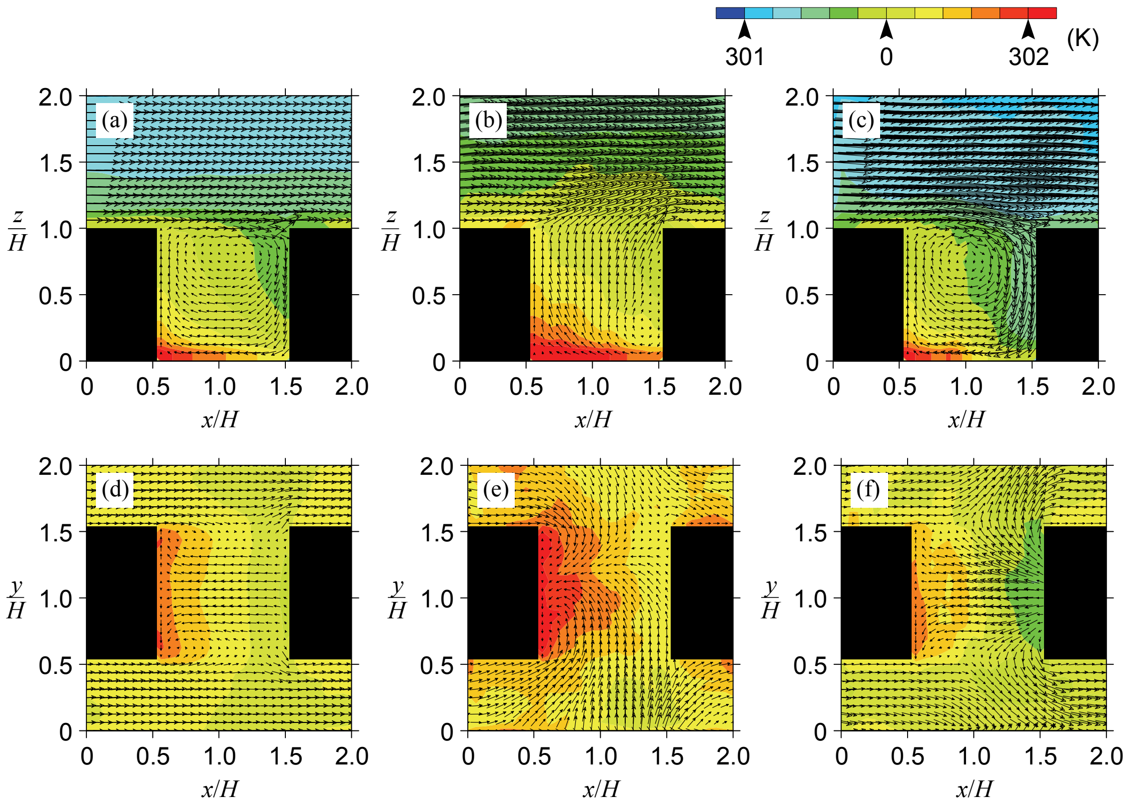

Figure 3 Conditional ensemble mean velocity and temperature fields on the vertical slice at the center of the cavity and horizontal slice at z=0.125H. (a), (d) full ensemble average, (b), (e) flushing, (c), (f) cavity eddy.

clearly related with the locations of the low speed streaks at 2H, which is drawn as grey regions, as the clusters of v converge to flow into the low speed streaks.

The high and low temperature regions at 0.125H (Figure 2d) are observed below the low and high speed regions at 2H, respectively. The higher temperature regions below the low speed streaks would be attributed to the horizontal flow convergence seen in Figure 2c. This convergent flow funnels the heated air near the ground into the bottom of the low speed streaks. It is also implied that the cooler temperature air from the high speed region at 2H impinge onto the bottom of the canopy.

4. FLOW STRUCTURE WITHIN THE CAVITY

We extracted two characteristic modes from the instantaneous flow structures in the square cavity, which are 'flushing' and 'cavity-eddy' events. In a flushing event, most of the area of the cavity is occupied by upward motion (Takimoto et al, 2010), which is numerically defined as "local upward velocity exceeding the local horizontal velocity at more than 55 % of the area of the vertical slice at the centre of the cavity". In a cavity-eddy event, a vortical motion, as seen in their ensemble structure, develops in the cavity. This is defined as, "the magnitude of downward velocity exceeding the magnitude of scalar velocity, which is averaged among the cavity, at more than 70 % of the area that is a quarter of the cavity nearby the windward wall on the vertical slice at the center of the cavity". These events are analyzed by conditional averaging, and the relationship with the turbulence structures in the upper layer was examined.

4.1 *Conditional averaged flow structures*

Figure 3 shows the conditional mean velocity vectors and temperature distributions on the x-z plane at the center of the cavity, and on the x-y plane at the height of 0.125H.

The full ensemble mean structure (Figures 3a, d) shows that there is vortical motion in the cavity as observed in several laboratory experiments (e.g. Uehara et al. 2004; Takimoto et al. 2010). The temperature is relatively higher at the bottom of the leeward wall due to the stagnation of the heated air at the bottom, and is lower at the top of the windward wall since the relatively cooler air above the canopy penetrates into the cavity by the cavity vortex.

In the flushing event, most of the area of the cavity is occupied by upward motion (Figure 3b). The spanwise flow is converging into the cavity (Figure 3e) although this convergent motion becomes weaker with increasing height (not shown). This strong convergence causes the upward divergence that occurs in the entire cavity. The temperature in the cavity is higher than that of the full ensemble mean. This is because the flow convergence concentrates the heated air near the ground, and the vertical

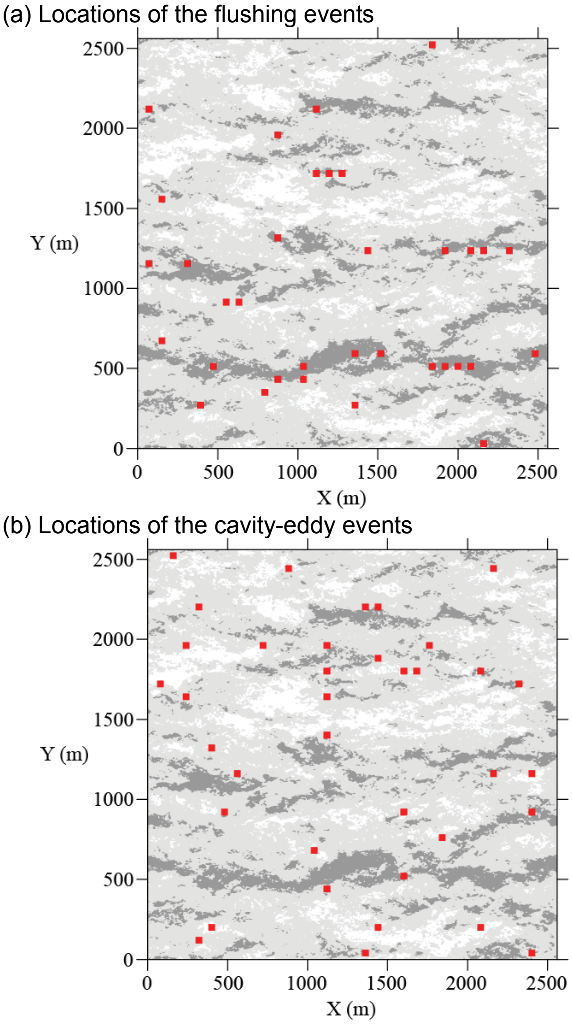

Figure 4 Locations of the flushing and cavity-eddy events plotted together with the u' at z=2H.

divergence prevents the penetration of the cool air from the upper layer into the canopy layer.

In the cavity-eddy event, there develops a stronger cavity eddy than in the full ensemble structure. This cavity eddy causes a strong downdraft at the windward wall (Figure 3c), and the horizontal divergence near the ground (Figure 3f) which is different from the flushing event. The strong cavity-eddy also causes the cool-air penetration from the top of the leeward wall more strongly than the full ensemble average. This can contribute to make the temperature lower in the cavity of the cavity-eddy relative to the other events.

4.2 *Relative locations of flushing and cavity-eddy events to the TOS in inertial sublayer*

The relative locations of flushing and cavity-eddy events with the TOS in the inertial sublayer are examined. Figure 4 shows the locations of the flushing and cavity-eddy events plotted together with the streamwise velocity fluctuation at 2H.

The flushing events are mostly observed below the low speed streaks at 2H (Figure 4a). The spanwise velocities converge into the low speed streaks, as seen in Figure 2c, and it invokes the upward divergence in the entire cavity. This is consistent with the conditional mean flow structure for flushing. The locations of cavity-eddy events seem to occur below the horizontal boundaries between the high and low speed regions at 2H (Figure 4b) although it is not as clearly shown as the case of the flushing event.

5. *INSTANTANEOUS FLOW CLASSIFICATION WITHIN A SQUARE CAVITY*

Assuming a semi-periodic nature of the cavity flow, instantaneous flow structure in a cavity is qualitatively classified into four modes based on the behavior of the vortex layer developed at the roof level. The use of the vortex layer for the classification is followed by the mixing layer analogy (MLA, Raupach et al. 1998) because this vortex layer roughly expresses the shear strength at the roof level, which is used for the scaling parameter in the MLA.

Figure 5 shows the typical flow structures which are visually classified by the shape of the vortex layer developed from the top of the windward wall; (1) fully-capped flow, (2) half-capped flow, (3) cavity-vortex flow, and (4) no-capped flow modes.

These modes are considered to be closely related to the mass exchange within and above the canopy layer for the following reasons. In the fully-capped flow, the exchange of air between in and above the canopy layer is poor since the flows are completely separated at the roof level. On the other hand, the flows are merging and freely exchange air mass within and above the canopy in no-capped flow mode. The flushing event is classified into the no-capped flow. The cavity-vortex flow has a strong cavity vortex, which takes the air above into the canopy. Spatially, half-capped flow might be followed by the no-capped flow.

6. *CONCLUSIONS*

We examined the relationship of instantaneous flow structures within and above the canopy layer from the numerical simulation. It is found that the flow in the canopy layer is well affected by the coherent structure of turbulence within the inertial sublayer, which is represented by the very large low speed steak structure. In respect to the momentum exchange in and above the canopy layer, large momentum transport is invoked by the passage of the very large low speed streaks.

ACKNOWLEDGEMENTS

This research was supported by the Ministry of Education, Science, Sports and Culture, Grant-in-Aid for Scientific Research (B): 21360233.

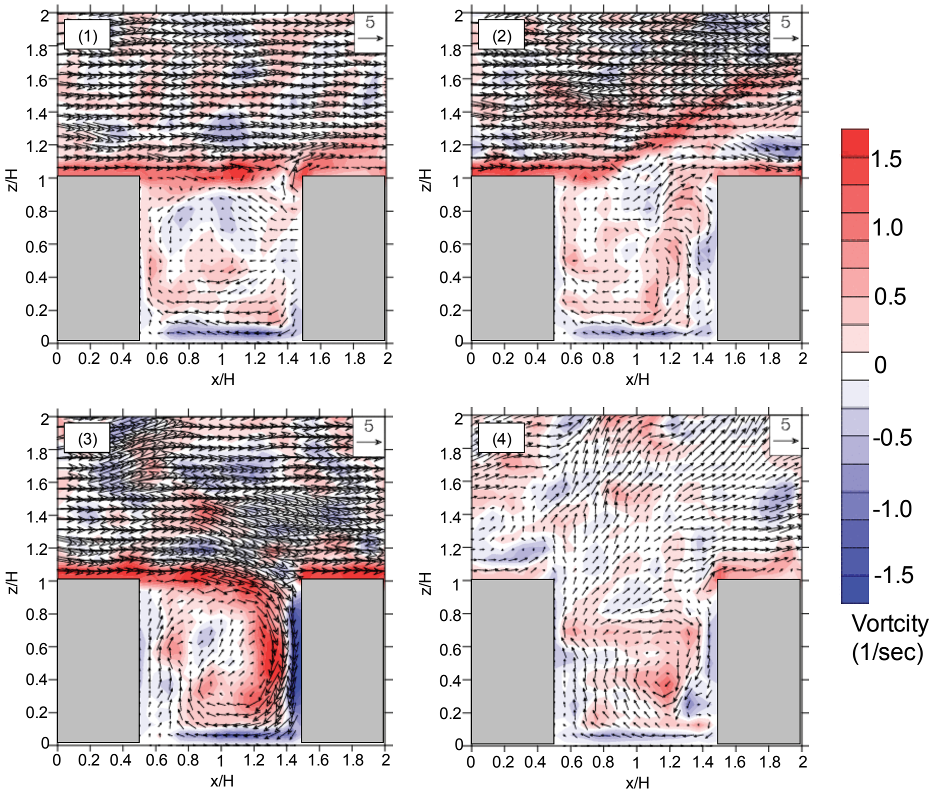

Figure 5 Instantaneous flow structures and the distribution of vorticity: (1) fully-capped mode, (2) open-capped mode, (3) cavity-eddy mode, (4) no-capped mode.

REFERENCES

Briscolini, M. and Santangelo, P. (1989): Development of the mask method for incompressible unsteady flows. *J. Comput. Phys.*, **84**, 57–75.

Castillo, M. C. L., Inagaki, A. and Kanda, M.: Inner and Outer Turbulence within the Inertial Sublayer of a Near-Neutral Atmospheric Flow Over an Urban-Like Surface. *Boundary-Layer Meteorol.* (in revision).

Christen, A., Gorsel, E. and Vogt, R., 2007: Coherent structures in urban roughness sublayer turbulence. *Int. J. Climatol.*, **27**, 1955–1968.

Coceal, O, Dobre, A. and Thomas, T. G. and Belcher, S. E., 2007: Structure of turbulent flow over regular arrays of cubical roughness. *J. Fluid Mech.*, **589**, 375–409.

Eliasson, I., Offerle, B., Grimmond, C. S. B. and Lindqvist, S., 2006: Wind fields and turbulence statistics in an urban street canyon. *Atmos. Environment*, **40**, 1–16.

Inagaki, A. and Kanda, M., 2008: Turbulent flow similarity over an array of cubes in near-neutrally stratified atmospheric flow. *J. Fluid. Mech.*, **615**, 101–120.

Inagaki, A. and Kanda, M., 2010: Organized structure of active turbulence developed over an array of cube within the logarithmic layer of atmospheric flow, *Bounday-Layer Meteorol.*, **135**, 209-228.

Kanda, M., Moriwaki, R. and Kasamatsu, F., 2004: Large eddy simulation of turbulent organized structure within and above explicitly resolved cubic arrays. *Boundary-Layer Meteorol.*, **112**, 343–368.

Letzel, M. O. 2007: High resolution Large-Eddy Simulation of turbulent flow around buildings. Ph. D. thesis, *Gottfried Wilhelm Leibniz Universität Hannover*.

Oikawa, S. and Meng, Y., 1995: Turbulence characteristics and organized motion in a suburban roughness sublayer. *Boundary-Layer Meteorol.*, **74**, 289–312.

Oke, T. R., 1987: *Boundary layer climates*. Routledge, London, 2nd edn., pp. 435.

Raasch, S. and Schröter, M., 2001: PALM – A large-eddy simulation model performing on massively parallel computers. *Meteorol. Z.*, **10**, 363–372.

Raupach, M. R., Finnigan, J. J. and Brunet, Y. 1996: Coherent eddies and turbulence invegetation canopies: the mixing-layer analogy. *Boundary-Layer Meteorol.*, **78**, 351-382.

Takimoto, H., Sato, A., Barlow, J. F., Moriwaki, R., Onomura, S. and Kanda, M.: PIV measurements of turbulent flow within an outdoor urban scale model and flushing motions in urban canopy layers. *Boundary-Layer Meteorol.*, (submitted).

Uehara, K., Murakami, S., Oikawa, S. and Wakamatsu, S., 2000: Wind tunnel experiments on how thermal stratification affects flow in and above urban street canyons. *Atmos. Environment*, **34**, 1553–1562.